

# Interpreting the 750 GeV diphoton signal as technipion

Antoni Szczurek

Institute of Nuclear Physics (PAN), Kraków, Poland

Rzeszów University, Rzeszów

Deep Inelastic Scattering 2016

Hamburg, Germany, April 11-15, 2016



# Outline

- 1 Generic production mechanisms
- 2 Vector-like TC model: a short overview
- 3 Production mechanisms of the signal
- 4 Background mechanisms in diphoton channel
- 5 Results



# Introduction

- Both **ATLAS** and **CMS** announced in December an observation of an intriguing enhancement in the diphoton invariant mass at  $M_{\gamma\gamma} \approx 750 \text{ GeV}$  in proton-proton collisions at  $\sqrt{s} = 13 \text{ TeV}$
- Many manuscripts on arXiv since the announcement. Many models beyond the Standard Model.  
*Higgs-like object, axion, technipion, etc.*
- What is the dominant **production mechanism** is a **speculation** at this stage.
- Different options:
  - (a) gluon-gluon fusion
  - (b)  $\gamma\gamma$  fusion
- We shall concentrate on the second option.
- We have some experience. A few processes considered by us so far:
  - $l^+l^-$
  - $c\bar{c}, b\bar{b}$
  - $W^+W^-$
  - $H^+H^-$



# Introduction

We shall consider two technicolor models (just examples):

- **vector-like TC** (Pasechnik, Beylin, Kuksa, Vereshkov)  
only fusion of (or decay into) electroweak bosons:  $\gamma\gamma$ ,  $\gamma Z$ ,  $ZZ$   
2 techniflavours, 3 technicolors
- **one family walking TC** (Farhi and Susskind, Matsuzaki, Yamawaki, et al.)  
gluon-gluon fusion dominates  
8 techniflavours, 3 or 4 technicolors  
used to interpret Higgs and 2 TeV diboson signal



# Production mechanisms

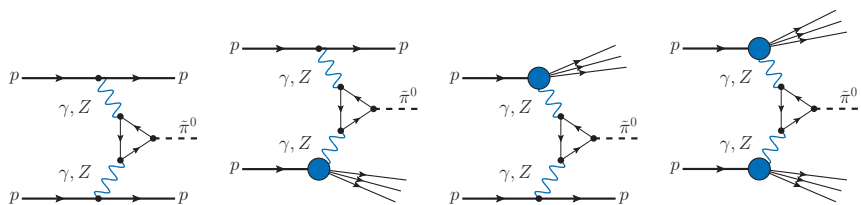


Figure: Diagrams of neutral technipion production via the  $\gamma\gamma$ ,  $\gamma Z$  and  $ZZ$  fusion.



# Production mechanisms

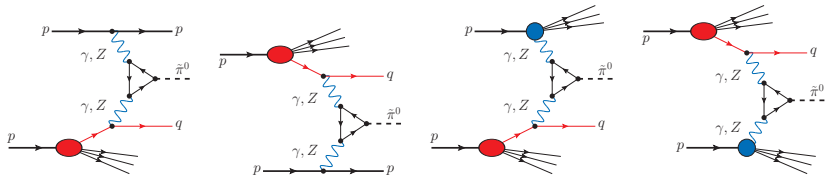


Figure: Technipion production via the  $2 \rightarrow 2$  partonic subprocesses.



# Production mechanisms

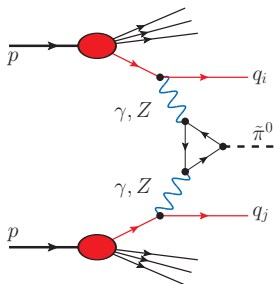


Figure: Technipion production via the  $2 \rightarrow 3$  partonic subprocesses.



# General information

Let us consider a single  $SU(2)_W$  doublet of Dirac techni-quarks

$$\tilde{Q} = \begin{pmatrix} U \\ D \end{pmatrix}, \quad (1)$$



# Decay widths

The techniquark-loop amplitude has the following form:

$$i\mathcal{V}_{\tilde{\pi}^0 V_1 V_2} = F_{V_1 V_2}(m_1^2, m_2^2, m_{\tilde{\pi}^0}^2; m_{\tilde{Q}}^2) \epsilon_{\mu\nu\rho\sigma} p_1^\mu p_2^\nu \varepsilon_1^{*\rho} \varepsilon_2^{*\sigma}, \quad (2)$$

$$F_{V_1 V_2} = \frac{N_{\text{TC}}}{2\pi^2} \sum_{\tilde{Q}=U,D} g_{V_1}^{\tilde{Q}} g_{V_2}^{\tilde{Q}} g_{\tilde{\pi}^0}^{\tilde{Q}} m_{\tilde{Q}} C_0(m_1^2, m_2^2, m_{\tilde{\pi}^0}^2; m_{\tilde{Q}}^2), \quad (3)$$

where  $C_0(m_1^2, m_2^2, m_3^2; m^2) \equiv C_0(m_1^2, m_2^2, m_3^2; m^2, m^2, m^2)$  is the standard finite three-point function,  $p_{1,2}$ ,  $\varepsilon_{1,2}$  and  $M_{1,2}$  are the four-momenta, polarization vectors of the vector bosons  $V_{1,2}$  and their on-shell masses, respectively, and neutral technipion couplings to  $U, D$  techniquarks are

$$g_{\tilde{\pi}^0}^U = g_{\text{TC}}, \quad g_{\tilde{\pi}^0}^D = -g_{\text{TC}}, \quad (4)$$



# Decay widths

$$F_{\gamma\gamma} = \frac{4a_{em} g_{TC}}{\pi} \frac{m_{\tilde{Q}}}{m_{\tilde{\pi}^0}^2} \arcsin^2\left(\frac{m_{\tilde{\pi}^0}}{2m_{\tilde{Q}}}\right), \quad \frac{m_{\tilde{\pi}^0}}{2m_{\tilde{Q}}} < 1, \quad (5)$$

$$F_{\gamma Z} = \frac{4a_{em} g_{TC}}{\pi} \frac{m_{\tilde{Q}}}{m_{\tilde{\pi}^0}^2} \cot 2\theta_W \left[ \arcsin^2\left(\frac{m_{\tilde{\pi}^0}}{2m_{\tilde{Q}}}\right) - \arcsin^2\left(\frac{m_Z}{2m_{\tilde{Q}}}\right) \right], \quad (6)$$

$$F_{ZZ} = \frac{2a_{em} g_{TC}}{\pi} m_{\tilde{Q}} C_0(m_Z^2, m_Z^2, m_{\tilde{\pi}^0}^2; m_{\tilde{Q}}^2), \quad (7)$$



## Decay widths

The decay width in a vector boson channel can be represented in terms of the effective couplings (3) as follows:

$$\Gamma(\tilde{\pi}^0 \rightarrow V_1 V_2) = r_V \frac{m_{\tilde{\pi}}^3}{64\pi} \bar{f}^3(m_1, m_2; m_{\tilde{\pi}}) |F_{V_1 V_2}|^2, \quad (8)$$

where  $r_V = 1$  for identical bosons  $V_1$  and  $V_2$  and  $r_V = 2$  for different ones, and  $\bar{f}$  is the normalized Källén function

$$\bar{f}(m_a, m_b; q) = \left( 1 - 2 \frac{m_a^2 + m_b^2}{q^2} + \frac{(m_a^2 - m_b^2)^2}{q^4} \right)^{1/2}. \quad (9)$$

For example in the VTC model for  $g_{TC} = 10$  and  $m_{\tilde{Q}} = 0.75 m_{\tilde{\pi}^0}$  one gets:

$$\Gamma(\tilde{\pi}^0 \rightarrow \gamma\gamma) = 5.136 \times 10^{-3} \text{ GeV}, \quad (10)$$

$$\Gamma(\tilde{\pi}^0 \rightarrow \gamma Z) = 4.376 \times 10^{-3} \text{ GeV},$$

$$\Gamma(\tilde{\pi}^0 \rightarrow ZZ) = 4.734 \times 10^{-3} \text{ GeV}.$$



# Decay width

The total decay width is a sum of the tree contributions:

$$\Gamma_{tot} = \Gamma(\tilde{\pi}^0 \rightarrow \gamma\gamma) + \Gamma(\tilde{\pi}^0 \rightarrow \gamma Z) + \Gamma(\tilde{\pi}^0 \rightarrow ZZ) . \quad (13)$$

The corresponding branching fractions are:

$$Br(\tilde{\pi}^0 \rightarrow \gamma\gamma) = 0.36 , \quad (14)$$

$$Br(\tilde{\pi}^0 \rightarrow \gamma Z) = 0.31 , \quad (15)$$

$$Br(\tilde{\pi}^0 \rightarrow ZZ) = 0.33 . \quad (16)$$



# Decay widths

Only at very large  $g_{TC} = 300-400$  one can reproduce the ATLAS quasi-experimental value  $\Gamma_{tot} \simeq 45 \text{ GeV}$  (only the ATLAS collaboration claims that the observed state is broad). The total width from the "experimental data" is rather speculative and thus should not be taken too seriously.

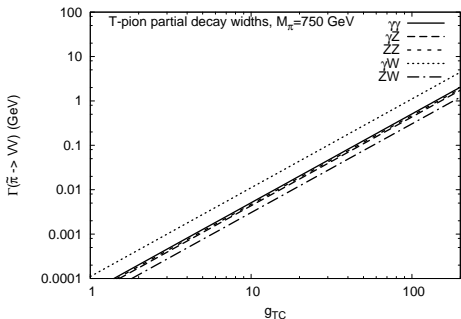


Figure: Decay width in GeV as a function of  $g_{TC}$  coupling constant. Here we have used our benchmark choice  $m_{\tilde{\Delta}} = 0.75 m_{\tilde{\Sigma}}^0$ .



2  $\rightarrow$  1 subprocess

$$\frac{d\sigma_{pp \rightarrow \tilde{\pi}^0}}{dy_{\tilde{\pi}^0}} = \frac{\pi}{m_{\tilde{\pi}^0}^4} \sum_{i,j} x_1 \gamma^{(i)}(x_1, \mu_F^2) x_2 \gamma^{(j)}(x_2, \mu_F^2) \overline{|\mathcal{M}_{\gamma\gamma \rightarrow \tilde{\pi}^0}|^2}, \quad (17)$$

where indices  $i$  and  $j$  denote  $i, j = \text{el or in}$ , i.e. they correspond to elastic or inelastic flux of equivalent photons, respectively.

Above  $y_{\tilde{\pi}^0}$  is rapidity of the technipion and

$$x_1 = \frac{m_{\tilde{\pi}^0}}{\sqrt{s}} \exp(y_{\tilde{\pi}^0}), \quad x_2 = \frac{m_{\tilde{\pi}^0}}{\sqrt{s}} \exp(-y_{\tilde{\pi}^0}). \quad (18)$$

In the leading-order collinear approximation the technipion is produced **with zero transverse momentum**

The elastic photon flux can be calculated using e.g. **Drees-Zeppenfeld parametrization**. To calculate inelastic contributions we use collinear approach with photon PDFs (**MRST(QED)**)



## 2 → 2 subprocess

$$\begin{aligned} \frac{d\sigma}{dy_3 dy_4 d^2 p_{t, \tilde{\pi}^0}} &= \frac{1}{16\pi^2 \hat{s}^2} \sum_i x_1 \gamma^{(i)}(x_1, \mu_F^2) x_2 q_{\text{eff}}(x_2, \mu_F^2) \overline{|\mathcal{M}_{\gamma q \rightarrow \tilde{\pi}^0 q}|^2}, \\ &+ \frac{1}{16\pi^2 \hat{s}^2} \sum_j x_1 q_{\text{eff}}(x_1, \mu_F^2) x_2 \gamma^{(j)}(x_2, \mu_F^2) \overline{|\mathcal{M}_{q\gamma \rightarrow \tilde{\pi}^0 q}|^2} \quad (19) \end{aligned}$$

where index “3” refers to technipion and index “4” refers to outgoing quark/antiquark. In this approach, transverse momenta of  $\tilde{\pi}^0$  and outgoing  $q/\bar{q}$  are strictly balanced. Here we have introduced effective parton distribution defined as:

$$q_{\text{eff}}(x, \mu^2) = \sum_f e_f^2 (q_f(x, \mu^2) + \bar{q}_f(x, \mu^2)). \quad (20)$$

The matrix element for the  $\gamma q \rightarrow \tilde{\pi}^0 q$  process including masses of quarks reads:

$$\mathcal{M}_{\gamma q \rightarrow \tilde{\pi}^0 q} = F_{\gamma\gamma} \varepsilon^{\mu\nu\kappa\alpha} p_{1\mu} p_{3\nu} \epsilon_{\kappa}^{(\gamma)}(p_1, \hat{n}_1) \frac{-ig_{a\beta}}{k^2} \bar{u}(p_4, \hat{n}_4) \gamma^\beta u(p_2, \hat{n}_2). \quad (21)$$



## 2 → 2 subprocess

The matrix element squared can be written in the Mandelstam variables  $(\hat{s}, \hat{t}, \hat{u})$  as

$$\overline{|\mathcal{M}_{\gamma q \rightarrow \tilde{\pi}^0 q}|^2} = \frac{1}{4} F_{\gamma Y}^2 \frac{2e^2}{\hat{t}^2} \left[ 2(\hat{s} - m_q^2)(k \cdot p_1)(k \cdot p_4) + 2(m_q^2 - \hat{u})(k \cdot p_1)(k \cdot p_2) - 4m_q^2(k \cdot p_1)^2 + \hat{t}(m_q^2 - \hat{s})(m_q^2 - \hat{u}) \right], \quad (22)$$

$$\overline{|\mathcal{M}_{q\gamma \rightarrow \tilde{\pi}^0 q}|^2} = \frac{1}{4} F_{\gamma Y}^2 \frac{2e^2}{\hat{t}^2} \left[ 2(\hat{s} - m_q^2)(k \cdot p_2)(k \cdot p_4) + 2(m_q^2 - \hat{u})(k \cdot p_2)(k \cdot p_1) - 4m_q^2(k \cdot p_2)^2 + \hat{t}(m_q^2 - \hat{s})(m_q^2 - \hat{u}) \right]. \quad (23)$$



## 2 → 3 subprocess

The cross section for the partonic  $qq' \rightarrow q\tilde{\pi}^0 q'$  process can be written as:

$$\sigma_{qq' \rightarrow q\tilde{\pi}^0 q'} = \frac{1}{2\hat{s}} \overline{|\mathcal{M}_{qq' \rightarrow q\tilde{\pi}^0 q'}|^2} \mathcal{J} d\xi_1 d\xi_2 dy_{\tilde{\pi}^0} d\phi_{12}, \quad (24)$$

where  $\phi_{12}$  is the relative azimuthal angle between  $q$  and  $q'$ ,  $\xi_1 = \log_{10}(p_{1t})$  and  $\xi_2 = \log_{10}(p_{2t})$ , where  $p_{1t}$  and  $p_{2t}$  are transverse momenta of outgoing  $q$  and  $q'$ , respectively.

The matrix element for the 2 → 3 subprocess was calculated as:

$$\begin{aligned} \mathcal{M}_{qq' \rightarrow q\tilde{\pi}^0 q'}(\hat{n}_1, \hat{n}_2, \hat{n}_3, \hat{n}_4) &= e^2 \bar{u}(p_3, \hat{n}_3) \gamma^\mu u(p_1, \hat{n}_1) \frac{-ig_{\mu\nu}}{\hat{t}_1} \\ &\times \varepsilon^{vv' a\beta} q_{1\alpha} q_{2\beta} F_{\gamma\gamma'} \frac{-ig_{v'\mu'}}{\hat{t}_2} \bar{u}(p_4, \hat{n}_4) \gamma^{\mu'} u(p_2, \hat{n}_2), \quad (25) \end{aligned}$$

often used in the literature in different context.



## 2 → 3 subprocess

For comparison, we shall also calculate the matrix element in the **high-energy approximation**:

$$\bar{u}(p', \hat{n}') \gamma^\mu u(p, \hat{n}) \rightarrow (p' + p)^\mu \delta_{\hat{n}' \hat{n}}. \quad (26)$$

We have also obtained a formula for matrix element squared and checked that it gives the same result as the calculation with explicit use of spinors. The total (phase-space integrated) cross section for technipion production could be alternatively calculated as:

$$\sigma_{pp \rightarrow \tilde{\pi}^0 jj} = \int dx_1 dx_2 \sum_{f_1, f_2} q_{f_1}(x_1, \mu^2) q_{f_2}(x_2, \mu^2) \hat{\sigma}_{f_1 f_2 \rightarrow f_1 \tilde{\pi}^0 f_2}(\hat{s}). \quad (27)$$

Limiting to  $\gamma\gamma$ -fusion processes only one can write:

$$\sigma_{pp \rightarrow \tilde{\pi}^0 jj}^{\gamma\gamma} = \int dx_1 dx_2 q_{eff}(x_1, \mu^2) q_{eff}(x_2, \mu^2) \hat{\sigma}_{qq \rightarrow qq \tilde{\pi}^0}^{eff}(\hat{s}), \quad (28)$$

where  $\hat{\sigma}_{qq \rightarrow qq \tilde{\pi}^0}^{eff}(\hat{s})$  is then the integrated cross section for the  $f_1 f_2 \rightarrow f_1 \tilde{\pi}^0 f_2$  subprocess with both fractional quark/antiquark charges set to unity.



## 2 → 3 subprocess

The above formula is not very efficient when calculating subprocess energy distribution. A more useful formula is:

$$\sigma_{pp \rightarrow \tilde{\pi}^0 jj} = \int dW \left( \sigma_{qq \rightarrow q \tilde{\pi}^0 q}(W) \int dx_d \left( \mathcal{J} q_{\text{eff}}(x_1, \mu^2) q_{\text{eff}}(x_2, \mu^2) \right) \right). \quad (29)$$

Above  $W = \sqrt{\hat{s}}$ ,  $x_d = x_1 - x_2$ , and  $\mathcal{J}$  is a Jacobian of the transformation from  $(x_1, x_2)$  to  $(W, x_d)$ . In practical calculation first partonic  $\sigma_{qq' \rightarrow q \tilde{\pi}^0 q'}$  (assuming elementary charges of quarks/antiquarks) is calculated as a function of  $W = \sqrt{\hat{s}}$  on a grid and then the convolution with parton distributions is done.



# Leading order VTC technipion signal in the diphoton channel

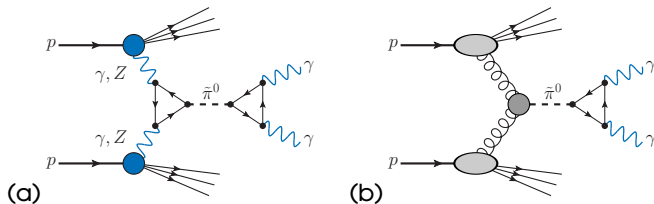


Figure: Leading order technipion signal in the diphoton channel in proton-proton collisions.



# Leading order VTC technipion signal in the diphoton channel

In the case of VTC technipion (Pasechnik et al.), the amplitude for the  $\gamma\gamma \rightarrow \tilde{\pi}^0 \rightarrow \gamma\gamma$  subprocess reads:

$$\begin{aligned}
 \mathcal{M}_{\gamma\gamma \rightarrow \tilde{\pi}^0 \rightarrow \gamma\gamma}(\hat{n}_1, \hat{n}_2, \hat{n}_3, \hat{n}_4) &= (\epsilon^{(\gamma)\mu_3}(p_3, \hat{n}_3))^* (\epsilon^{(\gamma)\mu_4}(p_4, \hat{n}_4))^* \\
 &\times \epsilon_{\mu_3\mu_4\nu_3\nu_4} p_3^{\nu_3} p_4^{\nu_4} F_{\gamma\gamma} \frac{i}{\hat{s} - m_{\tilde{\pi}^0}^2 + im_{\tilde{\pi}^0}\Gamma_{tot}} \\
 &\times \epsilon_{\mu_1\mu_2\nu_1\nu_2} p_1^{\nu_1} p_2^{\nu_2} F_{\gamma\gamma} \epsilon^{(\gamma)\mu_1}(p_1, \hat{n}_1) \epsilon^{(\gamma)\mu_2}(p_2, \hat{n}_2). \quad (30)
 \end{aligned}$$



# Leading order VTC technipion signal in the diphoton channel

The  $\Gamma_{tot}$  can be calculated from a model or taken from recent "experimental data". In the following we take the **calculated value** of  $\Gamma_{tot}$  and  $m_{\tilde{t}^0} = 750$  GeV. The mass scale of the **degenerate techniquarks**  $m_{\tilde{Q}}$  is another free parameter.

The cross section for the signal in this scenario is calculated then as:

$$\frac{d\sigma}{dy_3 dy_4 d^2 p_{t,y}} = \frac{1}{16\pi^2 \hat{s}^2} \sum_{ij} x_1 \gamma^{(i)}(x_1, \mu_F^2) x_2 \gamma^{(j)}(x_2, \mu_F^2) \overline{|\mathcal{M}_{\gamma\gamma \rightarrow \tilde{t}^0 \rightarrow \gamma\gamma}|^2}. \quad (31)$$

The factorization scale makes sense only in the case of dissociation of a proton. In the calculations we take  $\mu_F^2 = p_{t,y}^2$  for these cases.



## One-family walking technicolor model

In the [one-family walking technicolor model](#) ([Matsuzaki, Yamawaki et al.](#)) the branching fractions for the  $gg$  and  $\gamma\gamma$  decay channels are given as:

$$\Gamma(P^0 \rightarrow gg) = \frac{N_{TC}^2 a_s^2 G_F m_{P^0}^3}{12 \sqrt{2} \pi^3}, \quad (32)$$

$$\Gamma(P^0 \rightarrow \gamma\gamma) = \frac{N_{TC}^2 a_{em}^2 G_F m_{P^0}^3}{54 \sqrt{2} \pi^3}, \quad (33)$$

where  $a_s \equiv g_s^2/(4\pi)$  is the strong coupling constant,  $N_{TC}$  is the number of (techni)colors in the walking technicolor model. For  $N_{TC} = 3$  we get:

$$\Gamma(P^0 \rightarrow gg) = 1.2 \text{ GeV}, \quad \Gamma(P^0 \rightarrow \gamma\gamma) = 1.2 \text{ MeV}.$$

The decay into two gluons is, in this model, a dominant decay channel ([Matsuzaki, Yamawaki et al.](#)). The total decay width in the model is also much smaller than the 45 GeV reported (ATLAS:2015).

It is interesting that the model gives roughly correct size of the signal for  $N_{TC} = 3, 4$ , [without any additional tuning](#).



# Production mechanisms of background

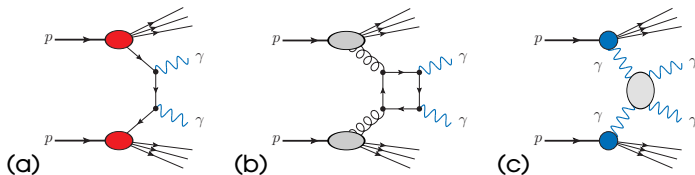


Figure: Background mechanisms of  $\gamma\gamma$  pairs production in proton-proton collisions.



## Background $q\bar{q}$ annihilation contribution

The lowest order process for diphoton production is quark-antiquark annihilation. The cross section for  $q\bar{q}$  annihilation can be written as:

$$\frac{d\sigma}{dy_3 dy_4 d^2 p_{t,\gamma}} = \frac{1}{16\pi^2 \hat{s}^2} \sum_f x_1 q_f(x_1, \mu_F^2) x_2 \bar{q}_f(x_2, \mu_F^2) \overline{|\mathcal{M}_{q\bar{q} \rightarrow \gamma\gamma}|^2}. \quad (35)$$

The formula for the matrix element squared for the  $q\bar{q} \rightarrow \gamma\gamma$  subprocess can be found in Berger et al. In our calculation we include only **three quark flavours** ( $u, d, s$ ).



## Background $gg$ fusion contribution

For a test and for a comparison we also consider the gluon-gluon contribution to the inclusive cross section.

The photons produced in  $pp(\bar{p}) \rightarrow \gamma\gamma + X$  are expected to be dominantly produced by the quark-antiquark annihilation ( $q\bar{q} \rightarrow \gamma\gamma$ ) and by the gluon-gluon fusion ( $gg \rightarrow \gamma\gamma$ ) through a quark-box diagram. The latter process is important especially at low diphoton invariant masses in kinematic region with high gluon luminosity.

In the lowest order of pQCD the cross section for inclusive cross section can be written as

$$\frac{d\sigma}{dy_3 dy_4 d^2 p_{t,\gamma}} = \frac{1}{16\pi^2 \hat{s}^2} x_1 g(x_1, \mu_F^2) x_2 g(x_2, \mu_F^2) \overline{|\mathcal{M}_{gg \rightarrow \gamma\gamma}|^2}. \quad (36)$$

The corresponding matrix elements have been discussed in detail by Glover et al.



## Background $\gamma\gamma$ fusion contribution

The cross section of  $\gamma\gamma$  production via  $\gamma\gamma$  fusion in  $pp$  collisions can be calculated in the same way as in the parton model in the so-called equivalent photon approximation as

$$\frac{d\sigma}{dy_3 dy_4 d^2 p_{t,\gamma}} = \frac{1}{16\pi^2 \hat{s}^2} \sum_{ij} x_1 \gamma^{(i)}(x_1, \mu_F^2) x_2 \gamma^{(j)}(x_2, \mu_F^2) \overline{|\mathcal{M}_{\gamma\gamma \rightarrow \gamma\gamma}|^2}. \quad (37)$$

In practical calculations for elastic fluxes we shall use **parametrization proposed by Drees-Zeppenfeld**.

The loop-induced helicity matrix element for the  $\gamma\gamma \rightarrow \gamma\gamma$  subprocess was calculated by using the `Mathematica` package **FormCalc** and the **LoopTools** library to evaluate one-loop integrals.

In numerical calculations we include box diagrams with leptons, quarks as well as with  $W$  bosons. At high diphoton invariant masses the inclusion of diagrams with  $W$  bosons in loops is crucial.



# Total cross section

Table: Cross section in fb for neutral technipion production at  $\sqrt{s} = 1.96, 7, 13, 100$  TeV for different contributions. We assume  $g_{TC} = 10$  and  $m_{\tilde{Q}} = 0.75 m_{\tilde{t}^0}$ .

Component	1.96 TeV	7 TeV	13 TeV	100 TeV
$2 \rightarrow 1$ (in-in)	1.37E-3	0.16	0.55	8.08
$2 \rightarrow 1$ (in-el)	0.22E-3	0.05	0.15	1.88
$2 \rightarrow 1$ (el-in)	0.22E-3	0.05	0.15	1.88
$2 \rightarrow 1$ (el-el)	0.03E-3	0.01	0.04	0.42
<b><math>2 \rightarrow 1</math>, sum of all</b>	<b>1.84E-3</b>	<b>0.27</b>	<b>0.89</b>	<b>12.26</b>
$2 \rightarrow 2$ (in-in), two diagrams	0.74E-3	0.14	0.49	7.69
$2 \rightarrow 2$ (in-el) and (el-in)	0.13E-3	0.05	0.19	2.93
<b><math>2 \rightarrow 2</math>, sum of all</b>	<b>0.87E-3</b>	<b>0.19</b>	<b>0.68</b>	<b>10.62</b>
$2 \rightarrow 2$ , sum of all, $p_{t,jet} > 10$ GeV			0.43	8.03
$2 \rightarrow 2$ , sum of all, $p_{t,jet} > 20$ GeV			0.35	6.99
$2 \rightarrow 2$ , sum of all, $p_{t,jet} > 50$ GeV			0.25	5.42
<b><math>2 \rightarrow 3</math></b>	<b>0.14E-3</b>	<b>0.09</b>	<b>0.46</b>	<b>16.71</b>
$2 \rightarrow 3$ , $p_{t,jet} > 10$ GeV			0.04	1.41



# Rapidity distribution

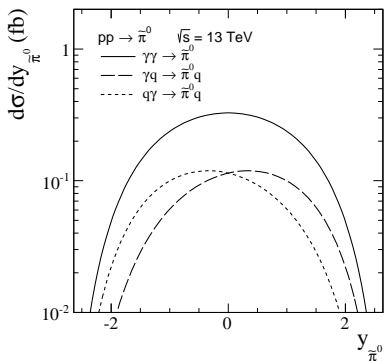


Figure: Distribution in rapidity of neutral technipion for all partonic subprocesses for the  $pp \rightarrow \tilde{\pi}^0$  at  $\sqrt{s} = 13 \text{ TeV}$ . In the calculation we take  $g_{TC} = 10$ ,  $m_{\tilde{\pi}^0} = 750 \text{ GeV}$ ,  $m_q = 1 \text{ MeV}$  (for all flavours),  $m_{\tilde{Q}} = 0.75 m_{\tilde{\pi}^0}$  (for both techni-flavours).



# Integration variables

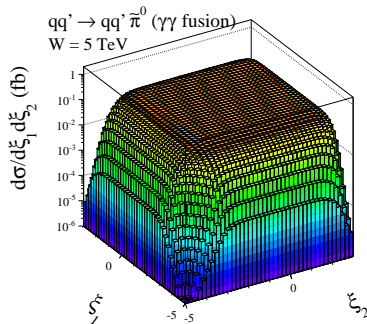
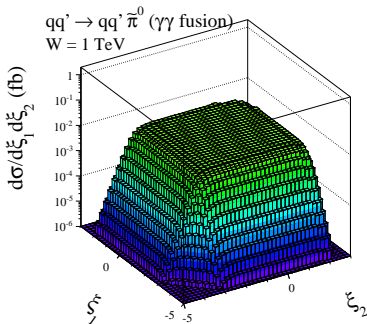


Figure: Differential  $qq' \rightarrow q\pi^0 q'$  cross section (unit charges) as a function of  $\xi_1 = \log_{10}(p_{1t})$  and  $\xi_2 = \log_{10}(p_{2t})$  for two subprocess energies: (a) W = 1 TeV (left panel) and (b) W = 5 TeV (right panel). In this calculation we use  $g_{TC} = 10$  for example.



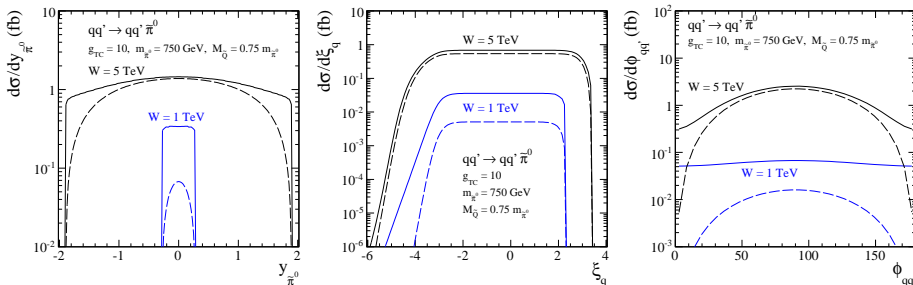
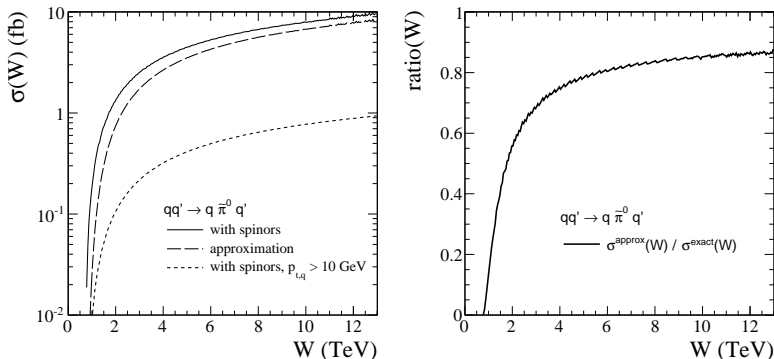
Some details of partonic  $2 \rightarrow 3$  calculations

Figure: Differential  $qq' \rightarrow q\tilde{\pi}^0 q'$  cross sections (assuming unit charges) for two subprocess energies  $W = 1$  TeV (blue lower lines) and  $W = 5$  TeV (black upper lines). The dashed lines were obtained in the [high-energy approximation](#) while the solid lines represent the **exact (with spinors)** calculations.



## Some details of partonic $2 \rightarrow 3$ calculations



**Figure:** Left panel: Total partonic  $qq' \rightarrow q\tilde{\pi}^0 q'$  cross section (unit charges) as a function of subprocess energy. In this calculation  $g_{TC} = 10$  was used for example. The solid line is for the calculation with spinors while the dashed line was obtained in the **high-energy** approximation. The dotted line corresponds to calculation for the **exact** case with the cut on both transverse momenta of (anti)quarks  $p_{t,q}, p_{t,q'} > 10$  GeV.



# Hadronic $2 \rightarrow 3$ cross section

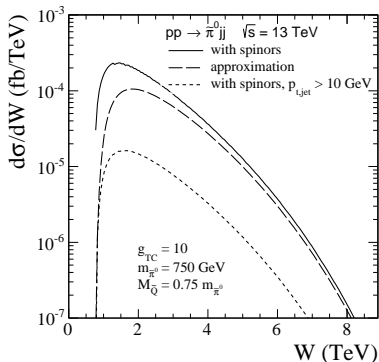


Figure: The distribution in the energy in the partonic subprocess for the  $pp \rightarrow \tilde{\pi}^0$  at  $\sqrt{s} = 13$  TeV. In this calculation we use  $g_{TC} = 10$  for example. The solid line is for the calculation **with spinors** while the dashed line was obtained in the **high-energy approximation**.



# Full hadronic cross section as a function of $g_{TC}$

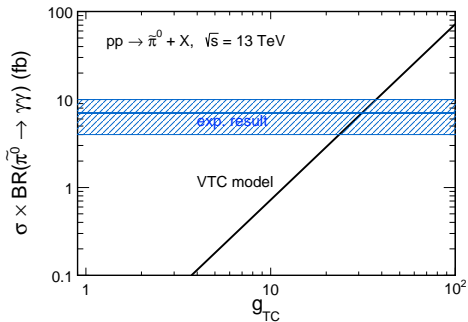


Figure: The dependence of the hadronic  $pp \rightarrow \tilde{\pi}^0$  cross section on  $g_{TC}$  together with **extracted by us experimental result**.



# Comparison with background contributions

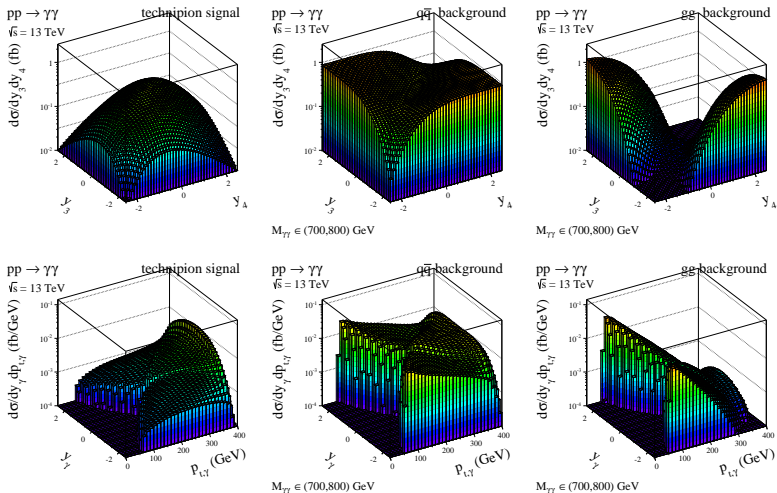


Figure: Two-dimensional distributions in pseudorapidity of photons (top panels) and



# Comparison with background contributions

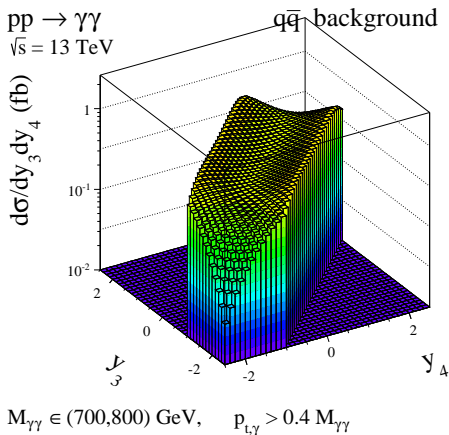


Figure: Two-dimensional distribution for the  $q\bar{q}$ -annihilation contribution at  $\sqrt{s} = 13$  TeV in the diphoton invariant mass range colored  $M_{\gamma\gamma} \in (700, 800)$  GeV with an extra limitations on both photon transverse momenta  $p_{t,\gamma} > 0.4 M_{\gamma\gamma}$ .



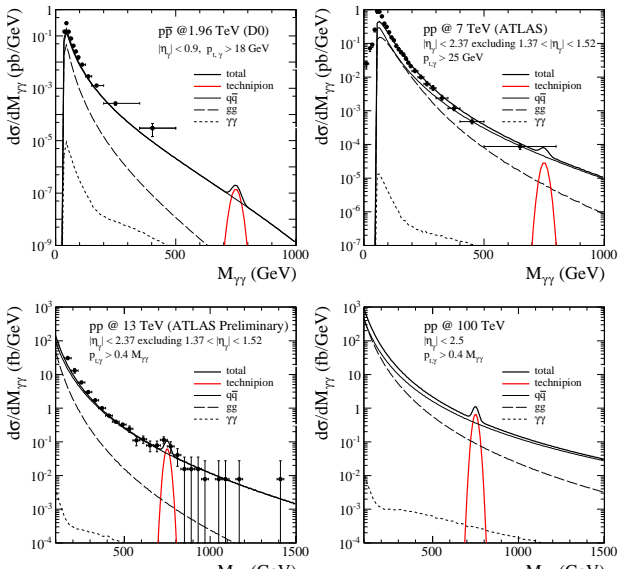
## Comparison with background contributions

The width in the VTC signal is small and we have to include **experimental resolution**. This is done by the **Gaussian function**:

$$\frac{d\sigma}{dM_{\gamma\gamma}} = \sigma_{\tilde{\pi}^0} \frac{1}{\sqrt{2\pi}\sigma} \exp\left(\frac{-(M_{\gamma\gamma} - m_{\tilde{\pi}^0})^2}{2\sigma^2}\right). \quad (38)$$



# Comparison with background contributions



# VTC signal with the existing data for dijets production

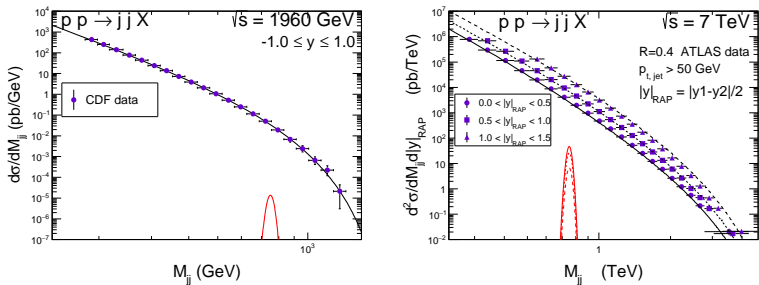


Figure: One-family walking technicolor isoscalar state (red lines). We show results of both CDF (left panel) and ATLAS (right panel) Collaborations. Please note different order of lines for the signal and the background.



# Conclusions

- Two technipion models have been considered in the context of the enhancement at 750 GeV.
- In the VTC model the techniquark-technipion coupling was adjusted to reproduce the strength of the signal at 13 TeV.
- The SM backgrounds for the diphoton final state have been considered.
- We have checked then the situation for other experiments and other collision energies.
- The signal is then below the SM backgrounds or below the limit set by the luminosity.
- Exclusive production  $pp \rightarrow pp\tilde{\pi}^0$  has been considered, but the cross section seems to be smallish.
- We have considered also the strength of the walking technicolor model (isoscalar object) for dijet production. The signal is significantly below the dijet background.
- Four-jet production channel may be interesting but the analysis is much more involved.



## General remarks

- In the moment none of the considered models can be excluded.
- In the walking TC model there should be also a **photon-photon signal** from **neutral isotriplet state**.
- Its mass was predicted at  $M_{\gamma\gamma} \sim 900 \text{ GeV}$ .  
But the cross section would be about **1000 smaller than for the isosinglet state** as it couples only to two photons (not to two gluons).
- Both the 750 GeV diphoton and 2 TeV diboson signals will be verified rather soon.
- **We have a chance to witness interesting time.**

